Hybrid model of quench propagation in coated conductors for fault current limiters

Arnaud Badel, Louis Antognazza, Mathieu Therasse, Markus Abplanalp, C Schacherer, Michel Decroux

Hybrid model of quench propagation in Coated Conductors for Fault Current Limiters

Arnaud Badel[1], Louis Antognazza[1], Mathieu Therasse[1,3], Markus Abplanalp[2], C. Schacherer[2] and Michel Decroux[1]

[1]University of Geneva DPMC, 24 quai Ernest-Ansermet, Geneva 1211, Switzerland
[2]ABB Corporate Research Centre, Dättwil, Switzerland

E-mail: arnaud.badel@unige.ch

Abstract
We developed a hybrid model of the quench propagation in coated conductors in current limitation condition. This model combines Finite Element Method to study the thermal behaviour of the coated conductors, and analytical calculation of the heat dissipation. We demonstrate that the evaluation of the heat dissipation can be conducted on a larger mesh than the FEM thermal problem. The results obtained with this model are in very good agreement with the experiments, without the need of using free parameters for adjustment. Parametric studies are then conducted to evaluate the influence of both the substrate thickness and the layer interfaces thermal properties, on the transition propagation behaviour. 3D simulations of a thin superconducting line placed on a wider substrate are also presented. Significant transverse heat propagation is observed in spite of the low thermal conductivity of the substrate, though this has little to no influence on the transition propagation along the line. These results are discussed in the context of FCL design.

1 Introduction

ReBCO Coated Conductors (the so-called 2nd generation HTS) are promising for resistive Fault Current Limiters (FCL) due to their high normal-state resistivity and current densities, which should lead to very compact FCL designs. Moreover, their price is decreasing and CC-based FCL devices will be significantly cheaper than bulk BSCCO FCL when the industrial stage will be reached. One of the major issues for an efficient use of CC in FCL, along with the difficulty to obtain homogeneous characteristics over long lengths, is the low normal zone propagation velocities (NZPV) that they display. These velocities are 2 orders of magnitude lower than what is observed with ReBCO deposited on sapphire [1], in the range of 10^{-2} to 10^{-1} m/s for current densities (J) slightly above the critical value J_c. In current limiting applications, low NZPV leads to slow increase of the total resistance. Finally, this slower establishment of the current limiting regime leads to an increased temperature excursion of the hot spot, which may be damaging for the conductor.

Slow NZPV in CC come from their poor thermal characteristics, with high thermal capacity and low thermal conductivity. However if this is established qualitatively, an accurate propagation model is needed to determine quantitatively the respective influences of the different thermal parameters on the

[3] Present address: European Organization for Nuclear Research / BE – RF, CERN CH-1211, Geneva 23, Switzerland

velocity: geometry of the layers, materials and interfaces characteristics. This information could be used to design FCL architectures making an optimal use of the conductors and / or optimize the conductor for this specific application.

Modelling CC conductor presents two challenges. From the electrical point of view, the strong non-linearity of the relation between electric field and current density in the superconducting dissipative state must be introduced. From the thermal point of view, the low thermal conductivity and the high thermal capacity of the layers make it impossible to consider the cross section as thermally uniform, especially considering the very high power density dissipated in the conducting layers. The very high aspect ratio of the layers also makes the modelling difficult using numerical methods such as FEM.

One dimensional transition propagation numerical models have been proposed, solving the heat diffusion equation along the CC length. They allow fast calculations but make assumptions about the thermal propagation in the CC cross section [2, 3, 4]. It is difficult in this case to discriminate the influence of the various layer parameters. On the contrary, 2D and 3D multi-physic models using FEM or FVM implement the electric and thermal equations at the microscopic scale [5]. However, the convergence issues coming from the power law implementation and the rapidly growing size of the problems make it difficult to extend such methods to long lengths of conductor and all the more to apply it to large scale application simulations.

2 Novel Hybrid model

In order to assert the influence of the layers characteristics on the ReBCO CC thermal behaviour in fault current limiter applications, we developed a new hybrid model for 2D and simple 3D simulations of CC in self-field. It combines analytical calculations to render the highly non-linear behaviour of the superconducting material, with numerical Finite Element calculations for a detailed evaluation of the thermal propagation in the CC layers. The possibility to simulate 3D geometries is presently limited to simple yet common cases, such as the study of transition propagation between adjacent conductors. For now, only the influence of the temperature on the current density repartition is considered, which is a reasonable assumption if the current is close-to or above the critical current.
The principle of the model is to use a thermal-only FEM model of the conductor, and calculate analytically the local heat dissipation, similarly to [6]. The particularity of our approach is that the evaluation of the heat dissipation is independent of the FEM problem, and may thus be conducted on a different scale from the FEM meshing. We demonstrate that this scale can be significantly higher while maintaining the accuracy, which allows faster and larger simulations.

2.1 Thermal model of the conductor

The thermal modelling of the conductor is made using COMSOL® software. A generic CC architecture is considered. It includes a substrate, an insulating buffer layer, the ReBCO layer and a silver shunt. The thermal conductivities and heat capacities of the layers and their temperature dependence are considered. From the thermal point of view, the silver shunt and the ReBCO layer can be merged into one (later called ReBCO/Ag layer) due to their thinness and the very good quality of the interface between. They will however be considered separately from the electrical point of view to evaluate the current sharing (cf. § 2.3). We suspect that the thermal properties of the interfaces between ReBCO and Buffer, and between Buffer and Substrate, may have a strong impact on the thermal behaviour of the CC. In order to account for these interfaces, an equivalent interface is added in the model between the substrate and the buffer layer. Finally, the thermal model makes the

assumption that there is no thermal exchange between the modelled conductor and the outside (cooling bath, thermal link, etc.). This assumption is supported by preliminary results obtained taking the exchange with the boiling nitrogen into consideration, without significant effect.

Equivalent interface evaluation. We reported recently a method [7] to measure an overall conductance regrouping the conductance of the ReBCO / Buffer interface and the Buffer / Substrate interface, but also the equivalent thermal conductance of the Buffer layer itself. As the buffer layer is considered separately in the proposed model, its influence must be deducted from the values obtained through this measurement technique in order to obtain the thermal conductance of the modelled equivalent interface.

ReBCO/Ag layer. In order to account for the localization of the heat dissipation along the conductor length, the ReBCO/Ag layer is split in blocks, each of them considered as an independent heat source. A schematic view of the resulting model geometry is presented Figure 1, for a 2D longitudinal cross section of a conductor. At each step of solving, the average temperatures on these blocks are calculated. The amount of heat produced in each block is then evaluated analytically in a function outside of the FEM problem, using the average temperature obtained. For 3D problems, the ReBCO/Ag layer is also split in along its width. For processing reasons, the number of blocks in the width of the tape must be constant along the conductor.

2.2 Evaluation of the heat dissipation

In the model, the substrate is electrically insulated from the ReBCO and Silver layers due to the buffer layer. In consequence, evaluating the heat dissipation in each block requires only the current densities in the silver and ReBCO layers and the resistivity of these layers. For ReBCO, two cases are considered: Above T_c it is in the normal state where it has an actual resistivity. In the superconducting state above J_c but below T_c, a power law is used to evaluate the flux flow resistivity varying with the temperature and the current density. Below $J_c(T)$ the superconductor is in the non-dissipative state and the resistivity is zero.

Power law. A modified formulation [8] is used to calculate the flux flow resistivity $\rho_{super}(J,T)$ for the superconductor in the dissipative state. With this formulation, the calculated resistivity truly reaches zero at $J_c(T)$.

$$\rho_{super}\left(J,T\right)=\rho_0\cdot\left(\frac{J}{J_c\left(T\right)}-1\right)^n \qquad \textbf{(1)}$$

where T_c is the critical temperature, $J_c(T)$ is the critical current at the temperature T. n and ρ_0 (respectively the order of the power law and the equivalent resistivity at $2.J_c$) are the two parameters that must be obtain through the characterization of the conductor.

The $J_c(T)$ curve can be derived from the measured J_c at one specific temperature, typically 77 K, through (2). This equation comes from the Ginzburg-Landau formulation [9] and was used successfully to predict the critical current of HTS wires in a wide range of temperature [10].

$$J_c\left(T\right)=J_{c0}\cdot\left(1-\left(\frac{T}{T_c}\right)^2\right)\cdot\left(1-\left(\frac{T}{T_c}\right)^4\right)^{1/2} \qquad \textbf{(2)}$$

where J_{c0} is the critical current expected at 0 K in self field.

The interest of this power law formulation is the reduced number of parameters that must be obtained through characterization ($J_c(77)$, n, ρ_0) and the invariance of these parameters in the studied range of temperature and current densities (see below Figure 3).

Current sharing. The current densities in the two conducting layers of each block are calculated within a Matlab® function, in which the power law formulation is implemented. This function contains the characteristic parameters $J_c(77)$, n and ρ_0. The temperature on the blocks is an input of this function, obtained from the thermal FEM calculation. As the current densities considered are high (close to or abvoe J_c) we consider that the current repartition in the conductor width is only influenced by the temperature.
For 2D problem considering the conductor along its length (Figure 1), the total current density passing through one block is constant. An iterative method is being used to evaluate the current sharing between the two conducting layers. It starts with 100 % of the current flowing through the ReBCO layer. It then evaluates the ReBCO resistivity and calculates the resulting current sharing. This new current distribution is used in the next step to evaluate again the resistivity of the ReBCO layer, and so on until the current distribution variation between two steps is lower than a given criterion. In order to insure the convergence of this iterative method, the current distribution at a given step is not obtained directly from the resistivity obtained in the previous step but from a pondered average obtained from the resistivities calculated in the two previous steps (Figure 2).
For 3D problems, we developed a modified evaluation function that calculate the current sharing between superconductor and resistive layers similarly as in 2D, but within another iterative loop that calculate the distribution of current in the width of the conductor. This function takes the average temperatures of all the blocks forming the ReBCO/Ag layer at a given cross-section, and evaluates the equivalent resistance of each of them considering a homogenous current density. The actual current densities in the different blocks are then obtained by iteration in a similar way as explained above for the 2D problem. This calculation of the current repartition along the width of the conductor only considers the influence of the temperature profile in the cross-section. Other influences of the 3D geometry, conductor path (turns, constrictions) or inhomogeneous magnetic flux density are not considered, which explains why the code is presently limited to simple 3D cases.

3 Results of Theva CC simulation

This model (2D version) has been used to simulate Theva Coated Conductor [11]. It consists of a hastelloy substrate on which an MgO insulating layer is deposited using ISD (inclined substrate deposition). On this MgO layer, DyBCO is grown by co-evaporation technique. A thin protective layer of silver is added on top.

3.1 Modelling data

The simulated 2D geometry represent a 20 mm long CC. As the problem is extended by symmetry with regards to its side on the left, the total simulated length is actually 40 mm. The simulation depth of the 2D problem, which represents the width of the modelled CC, is 3 mm.
In the model, the characteristics of each block forming the DyBCO/Ag layer can be defined independently, including the current density flowing through it. In order to maintain the continuity, this current density is the same in every block, except for the initial dissipating zone. This initial dissipating zone is a 400 µm-long length of conductor, at the left extremity of the modelled ReBCO/Ag layer, where the current density value is 1.5 times larger than elsewhere (Figure 3). This

increased current density reproduces the effect of a constriction in which the conductor width would be reduced to 2 mm. It initiates the transition of the CC. As the problem is symmetrized, this initial dissipating zone is actually 800 μm long and it is at the middle of the total 40 mm simulated length.
Electrical characterization was conducted on this conductor to obtain the power law parameters required by the model, following the methodology presented in [12]. A critical current density of $9\ 10^9$ A/m^2 has been measured, with a power law order n of 1.6 and an initial resistivity ρ_0 of 0.32 nΩ.m (Figure 4). The thermal and electrical characteristics of the modelled layers are interpolated from bibliography data in the range of 77 to 600 K. The extreme values are regrouped in Table 1. The equivalent interface conductance was derived from measurement using the new characterization method reported in [7]. The obtained value was 300 W/K/cm^2 (Table 1). Even if this value is higher than expected, it is considerably lower than the equivalent conductance of the buffer layer (11.10^3 W/K/cm^2 at 77 K). It will therefore have a stronger influence on the thermal behaviour.
In the simulations the current density was considered to stay constant in time. The simulations were stopped when the initial dissipating zone (hot spot) reached 600 K. This temperature is considered as an acceptable limit for the tape operation [13].

3.2 Simulated propagation velocity and heat dissipation

The length where the temperature exceeds 90 K is obtained from the FEM model for each time step, and used to derive the NZPV. Figure 5 shows the evolution of the propagation velocities with time, for a current density of 1.1 J_c and 1.78 J_c. For 1.1 J_c the obtained propagation velocity is constant, as it is assumed classically. However, for higher current densities such as 1.78 J_c, the propagation velocity tends to increase. This is probably due to the pre-heating of the whole length of the sample, which at such high current densities is in the dissipating state since the beginning of the simulation.
Apart from the temperature gradient, the localization of the heat dissipation can also be obtained from the model. Figure 6 displays the heat dissipation gradient in the first 3 mm of the simulated sample under 1.1 J_c when the hot spot reaches 600 K. The heat dissipation is expressed in power per surface of tape, taking into account the thickness of the dissipating layer (DyBCO/Ag). The maximum value reaches 1 kW/cm^2.

3.3 Influence of the modelling block size

In the proposed model, the heat dissipation in the DyBCO/Ag layer is evaluated on blocks having an adjustable length, larger than the FEM mesh. The dependence of the simulated propagation velocity with these block lengths is presented Figure 7, for a fixed FEM meshing of 10 μm along the modelled length (20 mm). These simulations were conducted for a current density of 1.1 J_c. It can be observed that the calculated value converge rapidly when the block length is reduced. For blocks shorter than 200 μm, the error is below 5 %, which validates the idea of evaluating the heat dissipation on a larger scale than the FEM meshing of the thermal problem. It is also observed that the value does not tend toward the limit monotonously but rather oscillates around it. This tends to prove that no systematic error is introduced by this macroscopic evaluation.

4 Agreement with experimental results

Propagation velocities on Theva CC were measured using small samples obtained by photo-lithography process. The transition is initiated by a constriction at the middle of the sample. This reduction of the width of the superconducting line leads to an increase of the current density by a factor 1.5, as it was considered in the simulations. The progression of the transition is deduced from voltage measurement along the sample length (Figure 8). The results of the 4 experiments that were

conducted show a significant dispersion, with measured NZPV ranging from 12.5 to 13.5 cm/s for a current density of 1.1 J_c (see the boundaries Figure 7). The mean value is around 13 cm/s, very close from the simulated values which converge to 12.8 cm/s. It demonstrates that it is possible to obtain an accurate propagation velocity using only standard characterization of the conductor and no free adjustment parameter.

The NZPV were measured for increasing current densities during the 4 experiments. The results are compared Figure 9 with the simulated values. The data range of the measurements is limited because the temperature increase for current densities in the range of 1.6 J_c is so high that the samples would be destroyed before measurement can be made. However, there is a fairly good agreement between simulation and experiments in the measured range. The results are also in good agreement with older measurement conducted on similar conductors, reported in [14].

Finally, we applied the model to YBCO deposited on sapphire, with electrical characteristics extracted from [14]. The simulated velocities range from 20 to 60 m/s under current densities varying from 1.5 to 2 J_c, with J_c being around 3 10^{10} A/m^2. These results are in good agreement with other available experiment data [14,15]. The good match between simulation results and experiments for both low and high thermal conductivity substrates proves that the proposed model is flexible enough to accurately render the behaviour of conductors with a wide range of characteristics.

5 Parametric CC simulations

Considering the good agreement between the existing Coated Conductors behaviour and the simulation results, this model can be used to extrapolate with a certain degree of confidence the velocities that would be obtained with other coated conductor architectures. Moreover, simulations require short processing times: it takes less than 5 minutes to determine the behaviour (NZPV, temperature rise) of a given CC architecture in given conditions.

The model was used to conduct parametric studies on two parameters that we believed to be critical regarding the thermal behaviour of the CC: Firstly the equivalent thermal conductance of the interfaces between the layers, secondly the thickness of the substrate itself. In order to have simulation results that can be compared from the application point of view, the electrical characteristics of the conductor remain must identical throughout the parametric studies. The properties and thicknesses of the DyBCO and Silver layers remain therefore unchanged.

5.1 Influence of substrate – buffer interface

As stated above in § 3.1, we recently reported measurements for the equivalent thermal conductance of the layer interfaces [7], at 300 W/K/cm². In order to determine the influence of this conductance value on the propagation velocities, we carried out parametric calculations, for values ranging from 1 to 10 000 W/K/cm². The results are presented Figure 10, for a current density of 1.1 J_c.

There is only slight variation of the NZPV when the interface conductance is above 100 W/K/cm^2. It proves that for the existing samples the interfaces could be considered perfect without introducing significant errors. A drastic increase of the propagation velocity can be observed when the equivalent conductance of the interfaces becomes lower than 40 W/K/cm², with velocities up to 7 m/s when the DyBCO layer is almost thermally decoupled from the other layers. However, the variation of the interface thermal conductance has also an effect on the temperature rise of the hot spot. This temperature rise will be faster if the interface conductance decrease, due to the weak thermal capacity of the superconducting line.

There is therefore a trade-off between quench propagation length and survivability of the CC: For low interface conductance the NZPV is higher and propagate the transition on longer length but the

survival time is shorter due to the faster hot spot temperature rise. For high interface conductance the temperature rise of the hot spot is slower and the survival time is longer, but the NZPV is lower which leads to smaller transited length. In order to determine if there is an optimal between these two extremes, Figure 11 shows the temperature profiles along the CC for different interface conductances. These temperature profiles are not taken at the same time, but for each of them at the moment where the hot spot reaches 600 K. An optimal zone can indeed be observed between 4 and 20 W/K/cm², where the transited length is longer. Further simulations will be necessary to determine whether this optimal zone exists in every configuration and experiments will be needed to determine if such optimal behaviour can indeed be obtained practically.

5.2 Influence of substrate thickness

As it was stated above, existing samples shows interface thermal conductances high enough to consider the YBCO layer perfectly coupled with the substrate. Figure 12 shows the influence of the substrate thickness on the propagation velocity, for a current density of 1.1 J_c. There is a continuous increase of the propagation speed for thinner substrate, as it was already observed by other groups [6]. At the same time the temperature profile tends to become stiffer, as shown Figure 13. In conclusion, reducing the thickness of the hastelloy substrate is not favourable for the survivability of the CC in FCL applications, as it leads to a fast rise of the hot spot temperature and an increased non-uniformity of the heat dissipation.

5.3 Effect of the substrate width

The 2D simulations makes the assumption that the superconducting layer has the same width than the substrate width. It is not the case in the experiment where the superconducting line has a width of 1 mm on a substrate that is 10 mm large. The agreement between the simulations and the experiments can therefore only be explained if the heat diffusion along the substrate width is small compared to the heat diffusion induced by the quench propagation along its length. In order to verify this assumption, simulations using the 3D version of the model were conducted for geometry closer to the one actually used for the measurements, consisting of a superconducting line (20 mm long, 1 mm wide) on a 20 mm per 10 mm substrate (Figure 14). The simulation was conducted with input data similar to the one used in 2D simulations, the transition being initiated in the middle of the central line. Figure 15 present the simulated temperature distribution (z axis) on the surface of the sample (x,y plane) at the moment where the hotspot reaches 600 K, with the simulated geometry superimposed. There is significant heat diffusion along the width of the sample, with the temperature reaching 90 K at up to 1 mm of the line on each side. This transverse diffusion of the heat softens slightly the temperature profile along the superconducting line. However, the NZPV is not affected by this different temperature distribution. It has a value of 12.7 cm/s for 1.1 J_c, almost equal to the 12.8 cm/s obtained in 2D.

6 First consideration for FCL design optimization

CC FCL takes usually the form of low inductance coils, in which the quench propagates only along the length of the conductor. It is commonly accepted that the worst operating condition for a FCL is an impedance fault leading to fault currents not so high above the critical current [16], in which case the conductor quenches only locally, which leads to little to no limitation of the current rise, and highly inhomogeneous heat dissipation. In order to limit the temperature rise in such condition, FCL designs usually include external shunt or extra normal conducting layers on the conductor in order to reduce the resistance per unit length. The maximal electric field usually accepted is around 0.5 V/cm, instead

of up to 10 V/cm if the CC was used without additional shunt and up to 40 V/cm for FCL using YBCO deposited on sapphire wafer [17]. This low equivalent resistivity per unit length increases the amount of conductor necessary to reach the desired limiting factor.

A solution to accept higher electric field with a given CC architecture could be the design of FCL geometries increasing the transition propagation velocity and therefore the homogeneity of the heat dissipation. We already proposed meander geometries with thermal links between the legs in order to initiate the transition on adjacent legs [18]. The results obtained from the 3D simulations of a superconducting line demonstrate that heat propagates significantly along the direction transverse to the superconducting line even if this phenomenon does not have an influence on the propagation velocity along the line. In consequence initiating the transition of adjacent lines, such as the legs of a meander, is possible if the distance between them is sufficiently small.

7 Conclusion

We developed a fast-processing model that is able to reproduce quantitatively the behaviour of CC conductor at the transition and under self-field, using standard conductor characterization and without the need of free adjustment parameters. It was used to determine the influence of both substrate thickness and interfaces conductance value on the transition propagation velocity and temperature uniformity. The results show that in general, a substantial increase of the transition propagation velocity cannot be achieved without at the same time lowering the heat dissipation uniformity, which is not favourable for FCL applications. It illustrates the need of developing new substrates with higher thermal characteristics in order to make compact and reliable CC-based FCL.

The proposed model is also able to simulate simple 3D geometries. The preliminary results show that there is non-negligible heat diffusion perpendicularly to the superconducting line, which may be useful for FCL made of CC plates, using meander geometries.

Future works will focus on adapting the model to different kind of conductors, such as architectures with electrical connections between substrate and shunt, multi-layer buffers, and so on. It will also aim at using the model to optimize meander designs taking advantage of this transverse heat propagation to obtain substantially higher equivalent propagation velocities.

Acknowledgment

This work was supported by the Swiss National Science Foundation through the National Center of Competence in Research MaNEP (Materials with Novel Electronic Properties).

References

[1] Heinrich A 2005 Quenching of superconductivity and propagation of the resulting normal phase in YBCO films *Supercond. Sci. Tech.* **18** 1354–59

[2] Daibo M, Fujita S, Haraguchi M, Iijima Y and Saitoh T 2011 Evaluation of the normal-zone propagation characteristics of REBCO coated conductors with laminated Cu tape. *IEEE Trans. Appl. Supercond.* **21**(3) 2428–31

[3] Pelegrin J, Martinez E, Angurel LA, Xie YY and Selvamanickam V 2011 Numerical and experimental analysis of normal zone propagation on 2G HTS wires. *IEEE Trans. Appl. Supercond.* **21**(3) 3041–44

[4] Celentano G et al 2009 Hot spot stimulated transition in YBCO coated conductors: experiments and simulations. *IEEE Trans. Appl. Supercond.* **19**(3) 2486–89.

[5] Chan W K, Masson P J, Luongo C and Schwartz J 2010 Three-dimensional micrometer-scale modeling of quenching in high-aspect-ratio YBa2Cu3O7-delta coated conductor tapes - part I: model development and validation *IEEE Trans. Appl. Supercond.* **20**(6) 2370–80.
[6] Roy F, Perez S, Therasse M, Dutoit B, Sirois F, Decroux M and Antognazza L 2009 Quench propagation in coated conductors for fault current limiters *Physica C* **469** 1462–66
[7] Antognazza L, Decroux M, Badel A, Schacherer C and Abplanalp M Measurement of the DyBCO / substrate thermal conductance in coated conductors. Submitted to *Supercond. Sci. Tech.*
[8] Decroux M, Antognazza L, Musolino N, de Chambrier E, Reymond S, Triscone J M, Fischer O, Paul W and Chen M 2001 Properties of YBCO films at high current densities: fault current limiter implications *IEEE Trans. Appl. Supercond.* **11**(1) 2046–49
[9] Poole C P, Farach H A, Creswick R J, Prozorov R 1995 *Superconductivity* (Academic press)
[10] Curtz N, Koller E, Zbinden H, Decroux M, Antognazza L, Fischer O and Gisin N 2010 Patterning of ultrathin YBCO nanowires using a new focused-ion-beam process *Supercond. Sci. Tech.* **23** 045015.
[11] http://www.theva.com/
[12] Therasse M, Decroux M, Antognazza L, Abplanalp M and Fischer O 2008 Electrical characteristics of DyBCO coated conductors at high current densities for fault current limiter application *Physica C* **468**(21) 2191–96
[13] Schwarz M, Schacherer C, Weiss KP and Jung A 2008 Thermodynamic behaviour of a coated conductor for currents above Ic *Supercond. Sci. Tech.* **21**(5) 054008
[14] Antognazza L, Therasse M, Decroux M, Roy F, Dutoit B, Abplanalp M, Fischer O 2009 Comparison between the behavior of HTS thin film grown on sapphire and coated conductors for fault current limiter applications *IEEE Trans Appl. Supercond.* **19**(3) 1960-63
[15] Antognazza L, Decroux M, Reymond S, de Chambrier E, Triscone J M, Paul W, Chen M and Fischer O 2002 Simulation of the behavior of superconducting YBCO lines at high current densities *Physica C* **372-376(**3) 1684–87
[16] Tixador P, Nguyen N T, Okada-Vieira H G and Ponceau R 2011 Impact of conductor inhomogeneity on FCL transient performance *IEEE Trans. Appl. Supercond.* **21**(3) 1194–97
[17] Antognazza L, Decroux M, Therasse M, Abplanalp M and Fischer O 2005 Test of YBCO thin films based fault current limiters with a newly designed meander *IEEE Trans. Appl. Supercond.* **15**(2) 1990–93
[18] Antognazza L, Decroux M, Therasse M and Abplanalp M 2011 Heat propagation velocities in coated conductors for fault current limiter applications *IEEE Trans. Appl. Supercond.* **21**(3) 1213–16

Figures

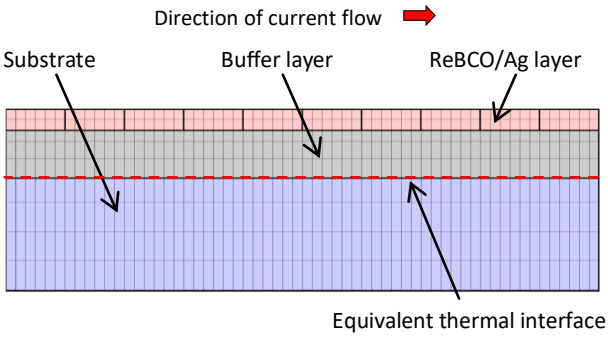

Figure 1: Schematic view of Model geometry in 2D

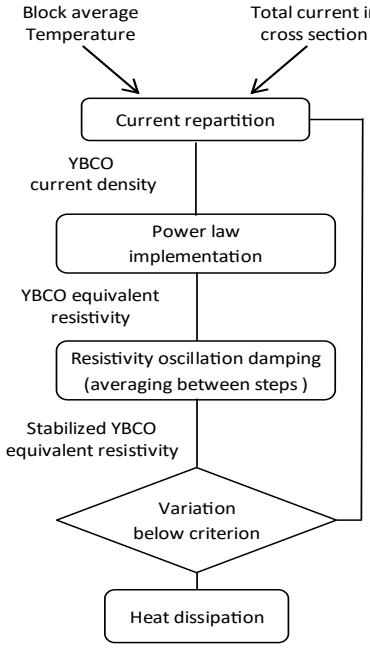

Figure 2: Current sharing iterative calculation

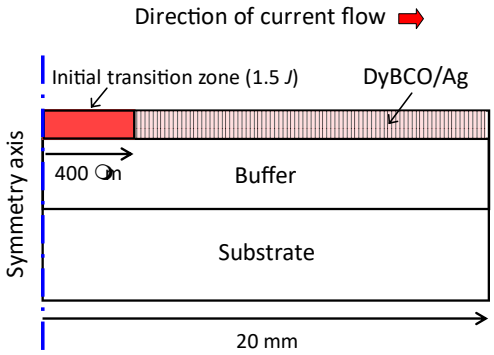

Figure 3: 2D Geometry for the simulation of transition propagation

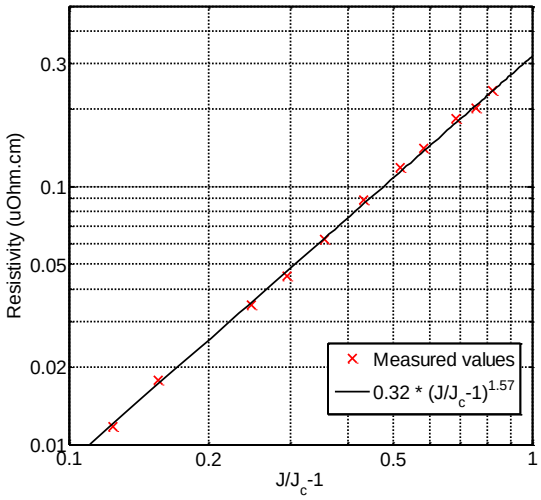

Figure 4: Electrical characterization of Theva coated conductor

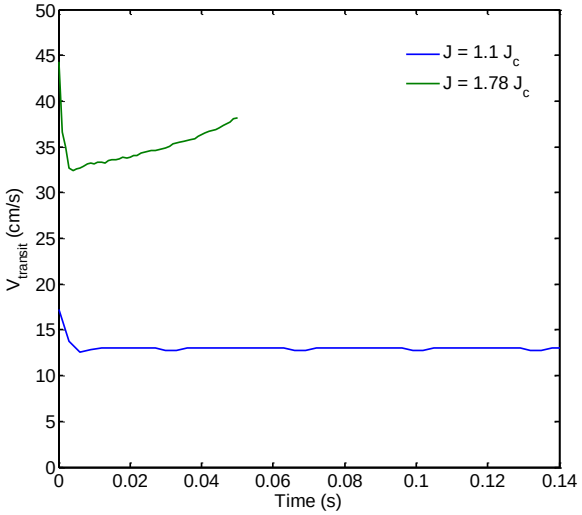

Figure 5: Propagation velocity evolution with time, for current density of 1.1 and 1.78 J_c

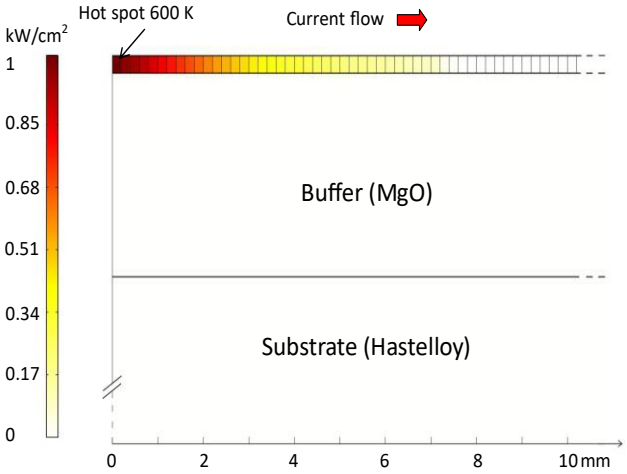

Figure 6: Heat dissipation per surface unit in the first 10 mm of the simulated length (Current density 1.1 J_c)

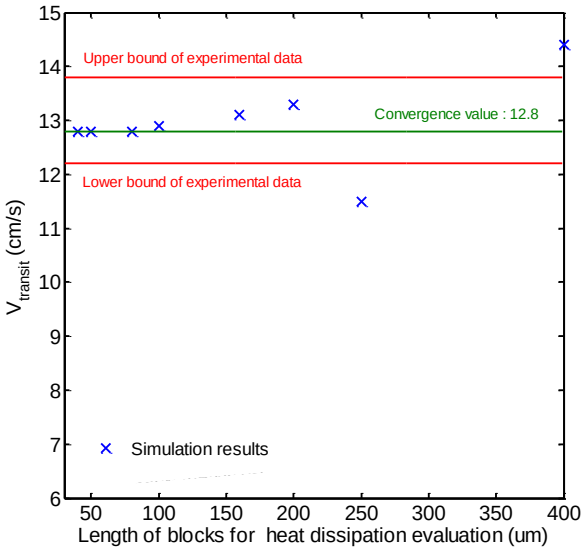

Figure 7: Dependence of the simulated NZPV with the length of the blocks used for the evaluation of the heat dissipation

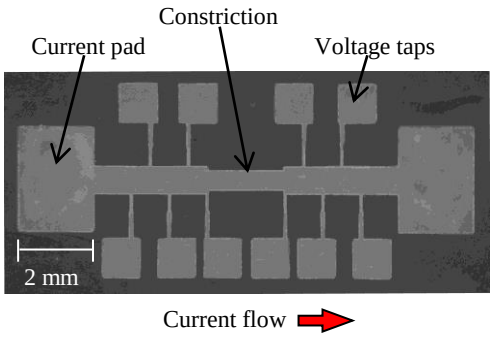

Figure 8: Theva sample etching for velocity measurement. The transition starts in the constriction at the middle of the sample, and its propagation is measured electrically.

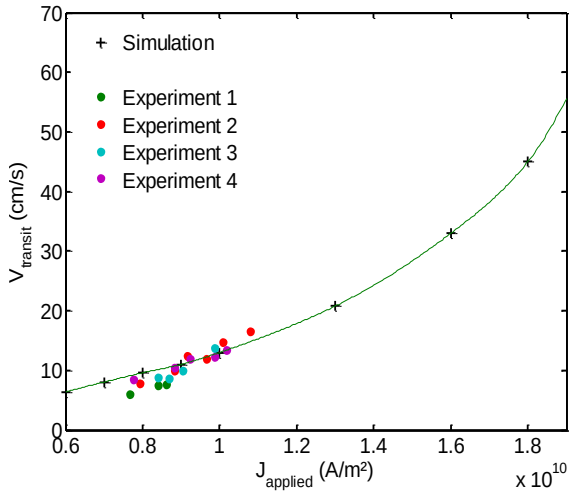

Figure 9: Comparison of simulated NZPV and experimental measurement for increasing current densities.

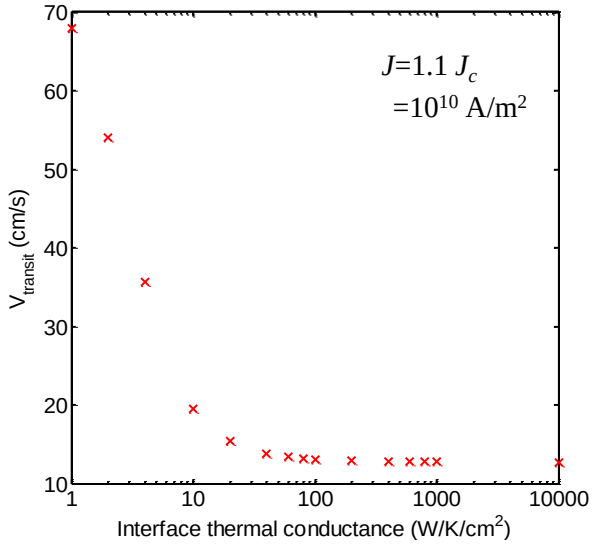

Figure 10: Simulated NZPV evolution with the equivalent interface thermal conductance

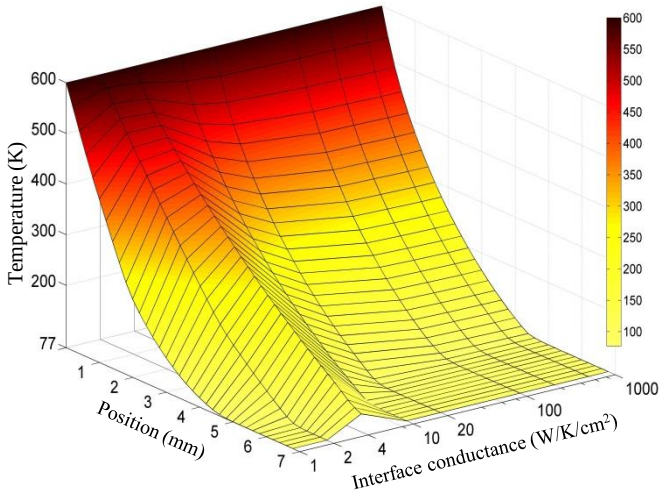

Figure 11: Temperature profile of the Ag/DyBCO layer when the hot spot reaches 600 K, for increasing values of equivalent surface conductance

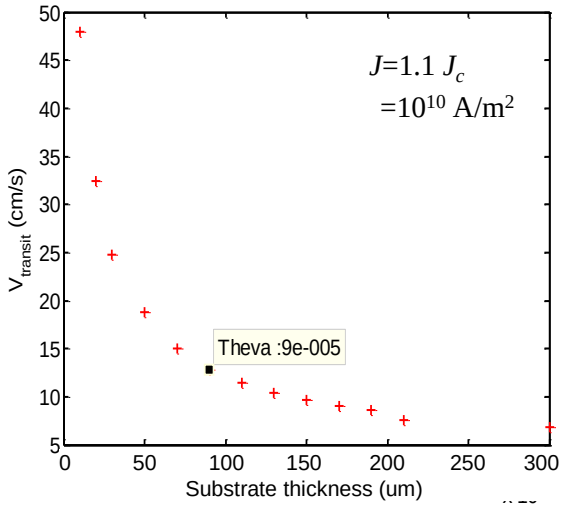

Figure 12: NZPV evolution with the substrate thickness

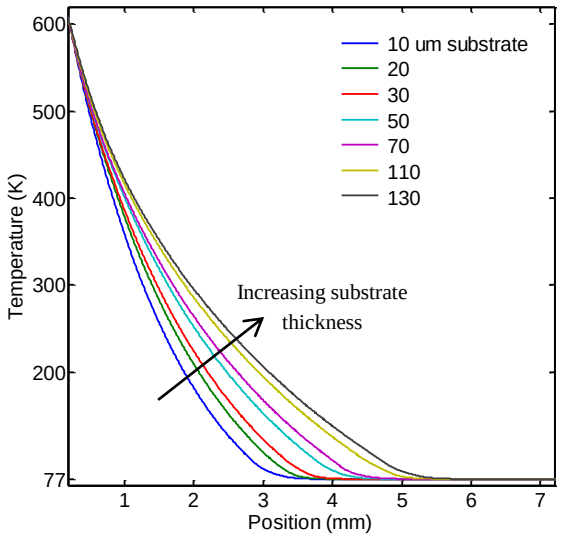

Figure 13: Temperature profile of the Ag/DyBCO layer when the hot spot reaches 600 K, for increasing values of substrate thickness

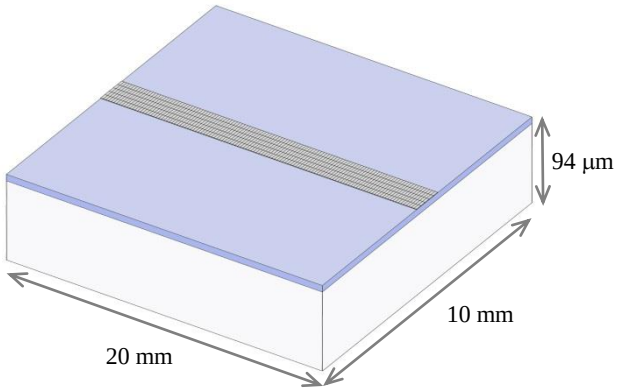

Figure 14: Simulated 3D geometry consisting of a 20 mm long 1 mm wide superconducting line on a 20 x 10 mm substrate + buffer.

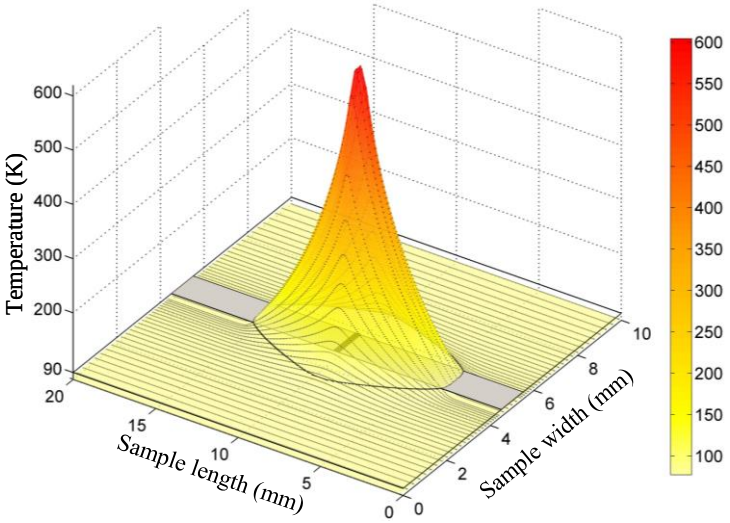

Figure 15: Simulated temperature distribution on the sample surface when the hot spot reaches 600 K. The superconducting line is superimposed in grey and the initial transition zone in black.

Tables

Layer	Thickness (μm)	Themal conductivity W/K/m		Heat capacity J/K/kg		Electrical resistivity nOhms.m	
		77	600	77	600	77	600
Silver	0.04	440	410	150	260	2.8	35
DyBCO (above Tc)	0.3	6.5	4.5	90	260	870	5800
MgO	4	445	37	50	1000	Irrelevant	
Hastelloy	90	7.8	17	170	460		
Conductance interface	0.001	3e-3		0			

Table 1 : model layer characteristics for Theva CC simulations